

Skip-SCAR: Hardware-Friendly High-Quality Embodied Visual Navigation

Yaotian Liu¹, Yu Cao², Jeff Zhang¹

Abstract—In ObjectNav, agents must locate specific objects within unseen environments, requiring effective perception, prediction, localization and planning capabilities. This study finds that state-of-the-art embodied AI agents compete for higher navigation quality, but often compromise the computational efficiency. To address this issue, we introduce "Skip-SCAR," an optimization framework that builds *computationally and memory-efficient embodied AI agents* to accomplish high-quality visual navigation tasks. Skip-SCAR opportunistically skips the redundant step computations during semantic segmentation and local re-planning without hurting the navigation quality. Skip-SCAR also adopts a novel hybrid sparse and dense network for object prediction, optimizing both the computation and memory footprint. Tested on the HM3D ObjectNav datasets and real-world physical hardware systems, Skip-SCAR not only minimizes hardware resources but also sets new performance benchmarks, demonstrating the benefits of optimizing both navigation quality and computational efficiency for robotics.

I. INTRODUCTION

Visual navigation is a core requirement in building autonomous robotic systems, with applications in domestic assistance, search-and-rescue operations, etc. Such real-world tasks require a mobile robot’s ability to extract information from its surroundings and determine its subsequent activity in an unseen world. Classical robotics navigation [1], [2] mainly builds on hand-crafted features or traditional algorithms [3]–[5]. Recent advancement of embodied AI techniques [6]–[8] empower the robots with better generalization ability in a unseen environments, where an embodied AI agent perceives, interacts and navigates within the physical environment based on its visual sensory input [9].

ObjectGoal navigation (ObjectNav) is a fundamental embodied visual navigation task that tests embodied AI agent’s both scene understanding and long-term memory [10], [11]. Consider navigating to a “toilet” in an unseen environment from a random location as shown in Figure 1, the task (episode) is marked successful if the agent stops near an object of the target category within a given time limit. To achieve this, the agent must leverage priors about environment layouts while searching for the target. Recent works [12]–[21] successfully pushed embodied AI agents towards remarkably higher navigation performance on standard ObjectNav benchmarks. State of the art embodied AI agent takes in its RGB-D observations, its own pose, and decomposes the task into ① semantic mapping, ② object probability prediction, ③ goal

selection, and ④ local re-planning stages (Figure 1 (a)). Such modular approach allows to tackle individual problems which are easier to solve, reuse the solutions across different tasks, and make the final processing pipeline more interpretable.

However, none of the prior works consider the computational cost, i.e., the compute latency and memory requirements when realizing embodied AI agents on real-world physical hardware. To understand this gap better, we performed detailed characterization of state of the art embodied autonomous agent (PEANUT [21]) running on modern CPU and GPU systems. Surprisingly, we observe that it can take upto 16 seconds for a 4-core 3.7GHz processor to compute the next action step for the embodied AI agent! Although GPU can significantly accelerate embodied AI agent’s “thinking speed”, our characterization unveils that **semantic segmentation (①)** and **local re-planning (④)** stages are the real-time performance bottleneck for ObjectNav (Figure 1 (b)); Furthermore, as shown in Figure 1 (c), the **object probability prediction (②)** stage peak the runtime memory footprint.

To this end, we introduce Skip-SCAR, an optimization framework that builds *computationally and memory-efficient embodied AI agents* to accomplish high-quality visual navigation tasks. To the best of our knowledge, our work is the first towards hardware-friendly embodied visual navigation. Our novelty and key contributions are:

- **A comprehensive end-to-end runtime profiling framework** that can benchmark the embodied AI agent’s real-time characteristics, memory consumption, along with their navigation quality on real hardware. Our framework can identify computational bottlenecks for real-world deployment.
- **A novel adaptive semantic mapping design** that opportunistically *skips* the redundant step computations during semantic segmentation and local re-planning without hurting the navigation quality. We observe that 40% of segmentation can be safely skipped to accelerate embodied visual navigation (Figure 1 (b)).
- **A lightweight object probability prediction DNN model (SCAR)** that achieves higher-quality object prediction while significantly compresses more than 70% of the target prediction model’s footprint and reduces 81% of its computations (Figure 1 (c)).
- **A thorough evaluation** of the proposed Skip-SCAR framework on large-scale real-world indoor HM3D dataset [22] and modern CPU/GPU systems. Skip-SCAR outperforms the existing best modular method [21] by $\sim 8\%$ in SPL and Soft-SPL, while running upto 34.4%

*This work was not supported by any organization

¹ Y. Liu and J. Zhang are with Ira A. Fulton Schools of Engineering, Arizona State University, Tempe, AZ 85281, USA

² Y. Cao is with the Department of Electrical and Computer Engineering, University of Minnesota, Minneapolis, MN 55455, USA

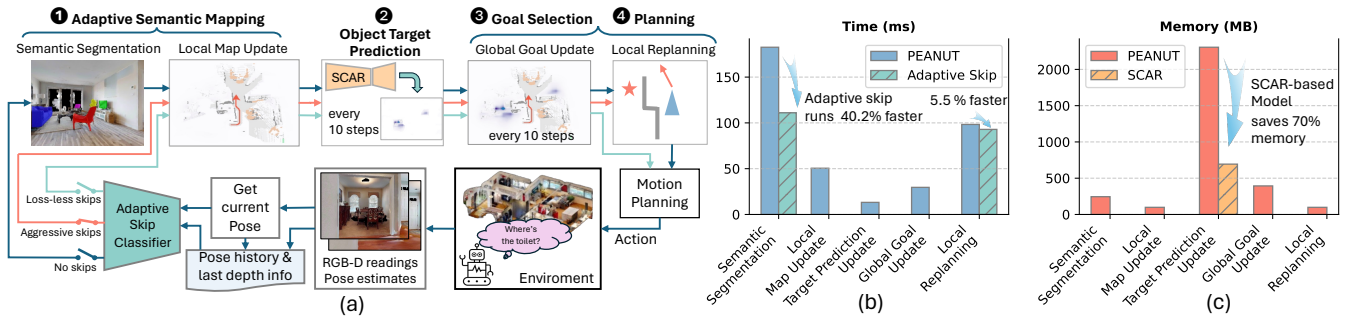


Fig. 1. **Overview of Skip-SCAR.** (a) At each step, the agent’s RGB-D observation and pose observations are used to update the incomplete global semantic map. This map is then used to predict a target object probability map, which is used to select long-term goals. Finally, an analytical local planner is employed to calculate the low-level actions necessary to reach the goal. (b) Bar plot of a single step computation time breakdown for Adaptive Skip vs. PEANUT on GPU system. The skip of 40.2% of semantic segmentation and 5.5% of local planning results in a corresponding reduction in their computation time. As target prediction and global goal update occur every 10 steps, we divide their respective times by ten. (c) Bar plot of a single step memory consumption breakdown for SCAR vs. PEANUT on GPU system. SCAR reduces the memory footprint by 70%.

faster and requiring 51.2% less memory.

II. RELATED WORKS

Embodied visual navigation research on ObjectNav task can be broadly classified into end-to-end learning methods and modular methods.

End-to-end learning methods [13]–[18] simplify the navigation process by mapping sensory inputs to motor outputs using deep learning models, typically involving convolutional neural networks (CNNs) and recurrent neural networks (RNNs). Recent advancements include Vision Transformers (ViTs) [17] and imitation learning with human demonstrations [18], [23]. ProcTHOR [13], which generates thousands of synthetic scenes and applied end-to-end RL with a CLIP backbone, stands out as a leading performer in this category. However, these methods require extensive training data and often suffer from poor generalization to new environments.

Modular methods break down the navigation task into phases—perception, planning, and control [19]–[21], [24]–[27]. This approach allows for targeted optimizations, enhancing efficiency and scalability. Stubborn [25] introduced a robust baseline for environmental exploration through a deterministic policy. SemExp [19] uses top-down semantic maps for environment understanding, while PONI [20] and PEANUT [21] predict target locations directly using semantic maps, avoiding the complexities of reinforcement learning. Our Skip-SCAR approach builds on top of PEANUT [21], further optimizing for computational and memory efficiency.

Sparse convolution techniques are essential for processing 3D point clouds, which are typically irregular and sparse. Vote3Deep [28] enhances sparsity through specialized convolutions. SparseConvNet [29] introduces submanifold sparse convolution, preserving active site locations and avoiding computations in inactive regions, while recently TorchSparse [30] improves the sparse convolution flow and provides higher efficiency on CUDA. Our proposed Skip-SCAR incorporate submanifold sparse convolution [29] to effectively manage environmental sparsity, significantly reducing computational operations and memory usage while speed up performance.

III. SKIP-SCAR APPROACH

Problem Formulation ObjectNav is an episodic embodied AI task where an agent is initialized at a random position and

orientation in an unseen environment and asked to find an instance of an object category (e.g., “chair”) using only its sensory input [10]. At each step, the agent receives a visual RGB-D observation and sensor pose reading, and takes navigational actions from: MOVE_FORWARD (0.25 m), TURN_LEFT (30°), TURN_RIGHT (30°), STOP. The episode is considered successful if the agent could reach within a certain distance (e.g., 1.0 m) of the target object and take the ‘stop’ action. Each episode has a fixed number of steps (500).

Goal of Our Approach The goal of Skip-SCAR is to build a computationally efficient embodied AI agent so that it can navigate to the object target quickly, both in terms of the navigation quality and its thinking (computation) speed.

Skip-SCAR evolves upon state-of-the-art modular approaches [19]–[21] for ObjectNav. As shown in Figure 1 (a), Skip-SCAR incorporates a novel adaptive semantic mapping design (section III-A) that opportunistically *skips* the redundant step computations during semantic segmentation and local re-planning to largely speed up embodied visual navigation (Figure 1 (b)). Furthermore, we propose a hybrid SparseConv-Augmented ResNet (SCAR) model for object target probability prediction ((section III-B)) with significantly lower model footprint and lesser computations (Figure 1 (c)).

A. Adaptive Skip Semantic Mapping Design

Baseline Semantic Mapping State-of-the-art embodied AI agents [19]–[21] uses RGB-D observations and the agent’s pose to construct a semantic map m_t which is shaped as $(4+N) \times H \times W$, where N represents the number of semantic categories. H, W is the height and width of the map. The first four channels denote the obstacle map, explored areas, current location of the agent and all previous locations, respectively. For the following N channels, the initial C channels are for target categories while the remaining $N - C$ channels cater to other categories. At each step, PEANUT [21], for instance, uses a pre-trained semantic segmentation model (Mask R-CNN [31]) to segment RGB-D images, and constructs a 3D point cloud from the depth observation with associated semantic label. Points within an agent’s height range are marked as obstacles. The point cloud is then converted into a voxel occupancy grid and summed across the height dimension to form an egocentric map. Using the agent’s pose, the egocentric map is transformed into an allocentric

coordinate system and integrated with existing semantic map. As shown in Figure 1 (B), baseline semantic mapping dominates 50% of the embodied AI agent’s total computation time.

Adaptive Skip Semantic Mapping Based on the agent’s sensory input, our approach opportunistically cuts off the baseline semantic segmentation processing via *lossless* and *aggressive* skips.

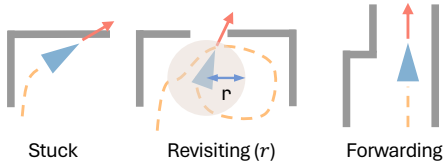


Fig. 2. Schematics of candidate skip scenarios, along with the agent’s navigation trajectory.

1) *Lossless skips*: If the agent’s RGB-D observation is exactly the same as previous steps, we can safely *skip* the semantic segmentation and *bypass* local replanning without losing any information. This scenario will happen when the agent’s current pose either stays unchanged (i.e., *Stuck*) or is same as a previous pose (i.e., *Revisiting*), as shown in Figure 2. By running all episodes of ObjectNav over different training maps, we empirically find that, the agent has 12.4% and 4.7% of its action steps in *Stuck* and *revisiting* that can be lossless skipped.

2) *Aggressive skips*: Our approach also allows the following aggressive skips when the agent’s RGB-D observations are highly similar to previous ones.

Approximate revisiting skip: we skip the agent’s semantic segmentation if its current location is within a revisit radius (r) from a historical location and if the agent’s pose angle remains the same. Empirically, we find that larger revisit radius (r) enables greater skip ratio and no navigation quality (SPL) drop when $r \leq 0.1m$, as shown in Figure 3.

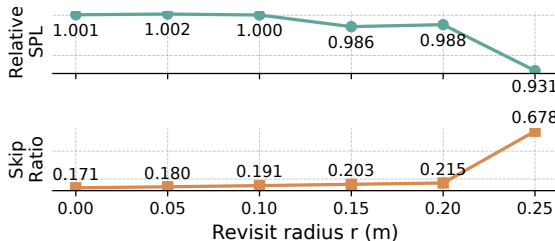


Fig. 3. Approximate revisiting skip under different revisit radius (r). SPL and skip ratio are normalized to no-skip baseline and averaged across 500 episodes in training set.

Forwarding skip: we skip the agent’s semantic segmentation if the semantic map update (Δm_t) is within a *Threshold*, i.e. the current RGB-D image does not add significant new information. Intuitively, when the agent walks straight in an indoor environment, visual input changes gradually unless it enters a new room. As our data shows, even if the agent naively skips all forwarding steps semantic segmentation (i.e., $\text{Threshold} \rightarrow \infty$), it can save 54.3% of computation with a 2.1% SPL drop.

However, during navigation, there is no way for the agent to compute the Δm_t if the current step semantic segmentation

is not processed. To solve this issue, we *formulate it as a forwarding skip prediction task* and train a machine learning classifier to predict the skip action based on the agent’s image depth input, as shown in Equation 1.

$$(L_m < \text{Threshold}) = J_\theta(D_n, D'_n) \quad (1)$$

J_θ is the judge model based on random decision forests [32] with weights θ . D_n and D'_n are the histogram (with n bins) of current and previous steps’ image depth inputs. L_m is the L1 loss of the new semantic map compared to the previous one. We use a Boolean value $L_m < \text{Threshold}$ as the label to indicate if the current semantic segmentation should be skipped, give an empirical *Threshold*. *For training*, we generate training labels from semantic maps gathered during agent interactions. *During inference*, the judge model is triggered when the agent’s previous action was FORWARD and decide if the current semantic segmentation should be skipped.

Adaptive Skip Classifier To unify all types of skip cases, we develop an adaptive skips classifier (see Algorithm 1) to enable real-time adaptive semantic mapping, which is incorporated into our embodied AI agent’s navigation pipeline (Figure 1).

Algorithm 1 Adaptive skip classifier

Input: Pose history p_{hist} , current pose p
Input: Current action a
Input: Current and last depth image d, d'
Output: $skip_type$

```

1: for  $p'$  in  $p_{hist}$  do
2:   if  $p = p'$  then ▷ Current pose is repeated
3:     return LOSSLESS
4:   else if  $|p, p'| < r$  then ▷ r is the revisit radius
5:     return AGGR_REVISIT
6:
7: ▷ Check forward skip
8: if  $a \neq \text{FORWARD}$  then
9:   return NONE
10:  $D_n, D'_n \leftarrow \text{binning}(d), \text{binning}(d')$ 
11: if  $J_\theta(D_n, D'_n)$  then ▷ Prediction indicates skip
12:   return SKIP_FORWARD
13: else
14:   return NONE

```

As outlined in Algorithm 1, we initially check if the agent’s pose is repeated or within the revisit radius r . If not and the current step is FORWARD, the agent calls prediction model J_θ for skip decision. We set a window size of 20 for pose history p_{hist} .

B. SparseConv-Augmented ResNet (SCAR) based High-Accuracy Target Probability Predictor

Baseline Target Probability Predictor The core of the embodied visual navigation pipeline is the explicit prediction model [12], [20], [21], [27], which represents the agent’s understanding of unexplored areas. PEANUT baseline [21] uses an encoder-decoder structure to produce a top-down probability map, in which each element contains the probability of each target category appearing in that location. Given

the agent’s incomplete semantic map $\mathbf{m}_t \in \mathbb{R}^{(4+N) \times H \times W}$ and a set of target categories $\mathcal{C} = \{1, 2, \dots, C\}$, PEANUT uses a *dense* ResNet-50 encoder to output the probability that an object of category c exists at a map location. However, we observe that, *PEANUT’s target probability predictor requires a large memory footprint (>2GB) and computations (>300 GFLOPs), as shown in Figure 1 (C)*. Furthermore, we also observe that PEANUT’s input semantic map \mathbf{m}_t is highly sparse. For instance, the proportion of non-zero elements across the spatial dimensions $H \times W$ is less than 10%!

SparseConv-Augmented ResNet (SCAR) Our approach adopts SparseConvNet [29] techniques to compress the irregular sparsity in the agent’s semantic map and eliminates the zero computations during the convolution operation. The key component of SparseConvNet is the submanifold sparse convolutional operation, which addresses the submanifold dilation problem by restricting the output of the convolution to the set of active input points, which can significantly reduce the computational complexity and memory requirements. In addition, SCAR also uses *strided (ST)* convolution to downsample the feature map since submanifold convolution inherently limits its ability to establish connections between distant points. To further tackle this limit, we augment it with a smaller, dense ResNet to process the input map in parallel to achieve highly accurate prediction.

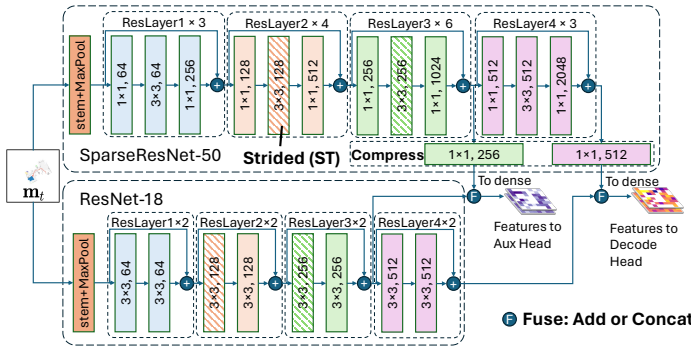


Fig. 4. **SparseConv-Augmented ResNet (SCAR)**. This is an example architecture SCAR-18-50. The SparseResNet-50 model follows the ResNet-50 architecture, with modifications where standard downsampling is replaced by convolutions with a kernel size of 3. The *strided* block indicates a stride size of 2 in the first block of each ResLayer, with no stride in subsequent blocks. *Compression* layers are 1×1 convolutions to align the channels of the sparse and dense. Sparse features are converted to dense format post-compression and *fused* with dense features. An auxiliary head aids training; only the decode head is active during inference. SCAR takes \mathbf{m}_t and outputs the target object prediction $\mathbf{y}_t \in \mathbb{R}^{C \times H \times W}$.

Figure 4 summarizes the overall SCAR architecture. SCAR processes the input semantic map \mathbf{m}_t by both SparseResNet and dense ResNet to extract sparse and dense features. A *compression layer* is added to align the channel number of the sparse features with that of the dense ones. The *fused* features are then fed into the decoder head for the subsequent processing.

Figure 5 visualizes the target prediction quality from ResNet-50 (PEANUT), standalone SparseResNet-50, SCAR-18-50, and the ground truth. As we can see naively adopting SparseConvNet fails to generate an accurate target prediction map, while our SCAR makes *the best* prediction.

SCAR Training and Inference SCAR follows [21] for



Fig. 5. Visualization of a sample target prediction output (e.g., a toilet) from different model candidates.

training data generation, loss function, and inference.

C. Prediction-Based Goal Selection and Local Planning

We adopt the same technique as previous works [19]–[21] for goal selection and planning. We compute the shortest path using the Fast Marching Method [33] and extract a waypoint from this path using the agent’s step distance. The global goal is selected considering both probability and distance. Replanning is done at every step. We use the same trap handler as [21] when the agent gets stuck.

IV. EVALUATION

We evaluate Skip-SCAR using standard Habitat ObjectNav Challenge setting [34] which include six goal categories and show it not only outperforms state-of-the-art embodied AI agents for navigation quality, but is also running faster and has a lower memory footprint.

Datasets We use large-scale HabitatMatterport3D (HM3D) dataset [22] in the Habitat simulator [11] for our experiments. HM3D consists of scenes which are 3D reconstructions of real-world indoor environments, split in training and test sets. Our training and test set consists of a total of 3971566 episodes from 800 maps and 2000 scenes (episodes) from 100 maps, respectively. The agent’s RGB-D observation resolution is set at 640×480 with a horizontal field view of 79 degrees. **Metrics** We use the following metrics for comparing the methods: **Success Rate (SR)** is the ratio of successful episodes. **SPL (Success weighted by Path Length)** is the success weighted by the length of the agent’s path relative to the oracle shortest path length [10], [34]. **SoftSPL (S-SPL)** is a modified version of SPL that track agent’s progress towards the goal, even when the episode fails [34]. **Skip Ratio** is the ratio for skipped semantic of the total steps for a navigation episode. **GFLOPs** (10^9 floating point operations), reports amount of computations.

Hardware Performance We run all experiments and measure the latency, memory consumption on the server with a 32-core AMD EPYC Milan 7313 Processor running at 3 GHz, 8 NVIDIA A5500 GPUs and 512 GB memory.

A. Adaptive Skip Semantic Mapping

Forwarding Skip Predictor Training We let an exploration agent roam 200 HM3D training episodes and extract the consecutive depth readings along with the corresponding semantic map difference (L1 loss) from 200 HM3D training scenes. We vary the map loss Threshold and revisit radius r and train the corresponding predictor using `BalancedRandomForestClassifier` from `imbalanced-learn` [35]. We use $n = 50$ bins in our training.

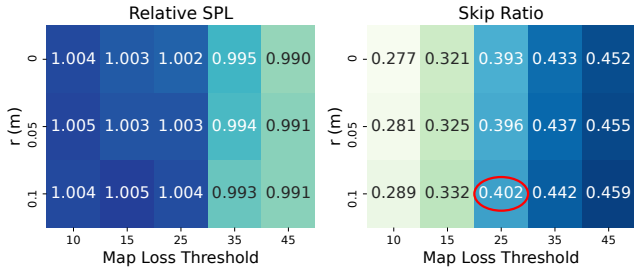


Fig. 6. Relative SPL and Skip Ratio of Adaptive Skip Classifier over PEANUT. Each grid shows the relative SPL or skip ratio achieved by the forwarding skip predictor, trained under a revisit radius and threshold pair.

Adaptive Skip Classifier Figure 6 reports the relative SPL, skip ratio, and relative time achieved by our proposed adaptive skip semantic mapping over PEANUT. We can see that our agent enables a max of 40.2% segmentation skips when the Threshold is 25, revisit radius is 0.1m without SPL drop.

TABLE I
ADAPTIVE SKIP VS. NAIVE SKIP

	Relative SPL \uparrow	Skip ratio	Step time \downarrow	Segmentation time \downarrow
Naive Skip	0.979	0.543	0.851	0.526
Adaptive Skip	1.004	0.402	0.814	0.616

We further compare our best adaptive skip model (highlighted in red circle from Figure 6) with a naive yet straightforward skip scheme (i.e., blindly skipping all FORWARD action’s segmentation) on the validation set. Note that all results are normalized to PEANUT in Table I. Although naive skipping allows greater skip ratio, it incurs a 2.1% SPL drop; Our adaptive skip model, on the other hand, achieves both better SPL and faster processing time. In particular, adaptive skip can reduce an average of 38.4% segmentation processing latency and can run a full action step 18.4% faster than PEANUT on the GPU.

Runtime Overheads. Our skip predictor only takes around 1.6 ms (which is 0.8 % of semantic segmentation) to make a prediction. The overhead is included in the time measurement for adaptive skip semantic mapping.

B. The Analysis and Performance of SCAR

SCAR Training Setting Our object prediction network uses a PSPNet [36] architecture with the proposed SCAR backbone and an auxiliary loss weight of 0.4. We use Adam optimizer with parameters $\alpha = 0.0005$ and $(\beta_1, \beta_2) = (0.9, 0.999)$, and a batch size of 8. The learning rate decay follows the "poly" policy [36]. To ensure consistency, we adhere to the training settings established in [21].

Why SCAR? Figure 7 illustrates the design space of the navigation quality (SPL) vs. computation cost (GFLOPs) for different object target prediction model architecture consideration discussed in Section III-B. We observe that (1) strided convolution (ST) improves SPL and reduces GFLOPs for both SCAR and dense ResNet18; (2) Both standalone

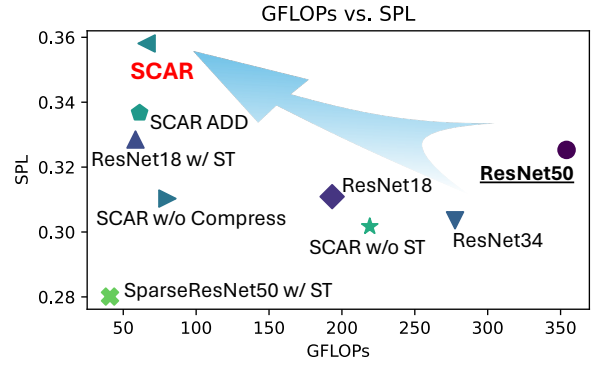


Fig. 7. Navigation quality (SPL) vs. Computation Cost (GFLOPs) for different object target prediction model architecture consideration discussed in Section III-B. ST stands for strided layers. Compress stands for compression layers, ADD means fused with addition.

SparseResNet-50 w/ ST and ResNet-18 w/ ST shows poor navigation quality. (2) The added compression layers yields a better SPL for SCAR; (3) Compared to the PEANUT (ResNet-50), SCAR achieves a 10.1% increase in SPL while reducing GFLOPs by 81.4%, highlighting the efficiency and effectiveness of SCAR. The results also validates our hypothesis on the inherent limits for SparseConvNet’s submanifold convolution.

Neural Architecture Search for SCAR To find a more memory-efficient SCAR, we perform neural architecture search (NAS) [37], [38] for SCAR. We use Optuna [39] for NAS optimization. The NAS explores the number of layers, the number of expansions for both SparseResNet and dense ResNet within SCAR, also the channel size of the decode head and the fuse methods between *concat* and *add*.

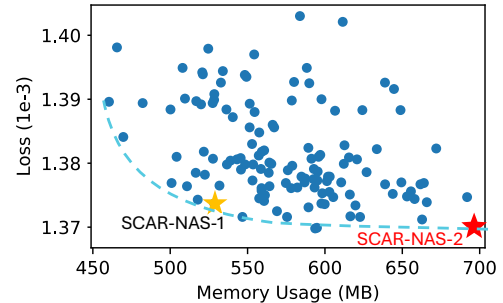


Fig. 8. Neural Architecture Search for SCAR. Training loss vs. SCAR memory footprint for the object target prediction model.

Figure 8 shows the tradeoff between training loss and scar memory footprint from our NAS. We compare both SCAR-NAS-1 and SCAR-NAS-2 models from the Pareto frontier with PEANUT’s ResNet-50 in Table II. SCAR-NAS-2 model outperforms the PEANUT in navigation quality (SPL) while significantly reduce its memory footprint (>70%), while at a similar baseline SPL, SCAR-NAS-1 enables even greater memory usage and computation savings.

C. End-to-End Performance for Skip-SCAR

The previous sections evaluates the benefits from standalone adaptive skip semantic mapping and standalone SCAR, respectively. This section applies both techniques and perform

TABLE II
DIFFERENT SCAR MODELS VS. PEANUT (RESNET-50)

	GFLOPs	Memory (MB)	SPL ↑
PEANUT	354.1	2305.4	32.5
SCAR-NAS-2	67.0 (↓ 81.1%)	693.9 (↓ 70.0%)	35.8 (↑ 3.3)
SCAR-NAS-1	42.7 (↓ 88.0%)	529.5 (↓ 77.1%)	33.3 (↑ 0.8)

end-to-end evaluation on the performance of the integrated Skip-SCAR embodied AI agent.

TABLE III
OBJECTNAV RESULTS ON HM3D VAL & TEST-STANDARD

#	Method	VAL			TEST-STANDARD		
		SPL	S-SPL	SR	SPL	S-SPL	SR
1	DD-PPO [15]	14.2	-	27.9	12.0	22.0	26.0
2	Habitat-Web [23]	23.8	-	57.6	22.0	26.0	55.0
3	OVRL-V2 [17]	28.1	-	64.7	29.0	-	64.0
4	ProcTHOR [13]	-	-	-	32.0	38.0	54.0
5	PIRLNav [18]	34.1	-	70.4	33.0	37.0	65.0
6	Stretch	-	-	-	34.0	38.0	60.0
7	ByteBOT	-	-	-	37.0	40.0	68.0
8	PEANUT [21]	30.8	33.9	60.6	33.0	36.0	64.0
9	SCAR (w/o skip)	33.3	36.6	60.5	34.2	37.8	60.8
10	Skip-SCAR	33.0	36.2	60.4	34.3	38.1	60.8

Navigation Quality We first benchmark Skip-SCAR against a spectrum of end-to-end and modular approaches, as well as strong but unpublished methods from the Habitat ObjectNav Challenge online leaderboard¹, which are highlighted in gray.

On VAL split, we evaluated Skip-SCAR on all 2000 episodes. Compared to the end-to-end baselines, Skip-SCAR surpasses DD-PPO [15] and Habitat-Web [23] with improvements of 131% and 37.8% in SPL, and 116% and 4.7% in SR, respectively. The recently proposed OVRL-V2 [17] achieves a 7.3% higher SR but has a 16.7% lower SPL than ours. PIRLNav [18], which leverages human demonstrations via imitation learning, shows superior performance in both SPL and SR compared to other modular methods. However, against the leading modular method PEANUT [21], Skip-SCAR improves the SPL and S-SPL scores by 8.1% and 7.9%, respectively.

We also evaluated Skip-SCAR on the TEST-STANDARD split, which hosts online and *is hidden for developers*. Excluding the unpublished ByteBOT, Skip-SCAR achieves the highest SPL and S-SPL. When compared to the state-of-the-art end-to-end RL method, ProcTHOR [13], our improvements are 6.9%, 0.3%, and 12.6% in SPL, S-SPL, and SR, respectively. Furthermore, our method does not require additional external training data as ProcTHOR does. Although PIRLNav shows better results on the VAL split, Skip-SCAR method outperforms it by 3.9% and 3.0% in SPL and S-SPL on the TEST-STANDARD split. Compared to the state-of-the-art modular method PEANUT, our SPL and S-SPL are higher

¹<https://eval.ai/web/challenges/challenge-page/1615/leaderboard/3899>

by 3.9% and 5.8%, respectively. We also completely surpass the second-ranked Stretch in all three metrics by 0.9%, 0.3%, and 1.3%.

TABLE IV
COMPUTATIONAL EFFICIENCY OF SKIP-SCAR VS. PEANUT

Hardware Platform	PEANUT [21]	Skip-SCAR
Single GPU Card	380.7 ms	309.9 ms (↓ 18.6%)
	3150.2 MB	1538.7 MB (↓ 51.2%)
4-thread CPUs	16.08 s	10.55 s (↓ 34.4%)

Computational Efficiency We evaluate the computational efficiency of Skip-SCAR on two modern hardware platforms: high performance (with a single A5500 GPU card), and embedded edge system (with a four-thread AMD CPUs).

Table IV shows the averaged wall clock time for the agent to finish one entire action step processing (which includes semantic mapping, object probability prediction, goal selection, and local re-planning stages). We observe that on the GPU system, Skip-SCAR runs 18.6% faster than PEANUT and consumes 51.2% less memory. Our CPU results also suggest that, the speedup of Skip-SCAR is more pronounced on resource-constrained devices (e.g., Raspberry Pi or micro-controllers).



Fig. 9. Example navigation episode using PEANUT and Skip-SCAR. The plots show the incomplete semantic map overlaid with the target probability prediction (the purple cloud). The agent was asked to locate the ‘chair’ in Episode 90 from HM3D VAL. Experiments are run on the GPU.

We demonstrate the overall navigation performance of Skip-SCAR’s in the full episode setting. Figure 9 shows the navigation trajectory performed by Skip-SCAR vs. PEANUT from the same starting location on the same map. Running on the GPU, Skip-SCAR agent successfully locates the object within tens of seconds, 7× faster than PEANUT.

V. CONCLUSION

This work introduced Skip-SCAR, a novel modular framework for ObjectNav that offers high-quality embodied visual navigation with high computational efficiency. Via the integration of SparseConv-Augmented ResNet (SCAR) and adaptive skips, Skip-SCAR significantly reduces memory usage and computational demands while maintaining high accuracy. Notably, Skip-SCAR outperforms state-of-the-art modular methods in both the HM3D dataset’s VAL and Habitat Challenge TEST-STANDARD splits in terms of both navigation quality and computation speed.

REFERENCES

- [1] T. Kruse, A. K. Pandey, R. Alami, and A. Kirsch, "Human-aware robot navigation: A survey," *Robotics and Autonomous Systems*, vol. 61, no. 12, pp. 1726–1743, 2013.
- [2] G. N. DeSouza and A. C. Kak, "Vision for mobile robot navigation: A survey," *IEEE transactions on pattern analysis and machine intelligence*, vol. 24, no. 2, pp. 237–267, 2002.
- [3] S. Thrun, "Probabilistic algorithms in robotics," *Ai Magazine*, vol. 21, no. 4, pp. 93–93, 2000.
- [4] A. Kosaka and A. C. Kak, "Fast vision-guided mobile robot navigation using model-based reasoning and prediction of uncertainties," *CVGIP: Image understanding*, vol. 56, no. 3, pp. 271–329, 1992.
- [5] M. Kabuka and A. Arenas, "Position verification of a mobile robot using standard pattern," *IEEE Journal on Robotics and Automation*, vol. 3, no. 6, pp. 505–516, 1987.
- [6] F. Zhu, Y. Zhu, V. Lee, X. Liang, and X. Chang, "Deep learning for embodied vision navigation: A survey," *arXiv preprint arXiv:2108.04097*, 2021.
- [7] B. Li, J. Han, Y. Cheng, C. Tan, P. Qi, J. Zhang, and X. Li, "Object goal navigation in embodied ai: A survey," in *Proceedings of the 2022 4th International Conference on Video, Signal and Image Processing*, 2022, pp. 87–92.
- [8] T. Zhang, X. Hu, J. Xiao, and G. Zhang, "A survey of visual navigation: From geometry to embodied ai," *Engineering Applications of Artificial Intelligence*, vol. 114, p. 105036, 2022.
- [9] M. Deitke, D. Batra, Y. Bisk, T. Campari, A. X. Chang, D. S. Chaplot, C. Chen, C. P. D'Arpino, K. Ehsani, A. Farhadi, L. Fei-Fei, A. Francis, C. Gan, K. Grauman, D. Hall, W. Han, U. Jain, A. Kembhavi, J. Krantz, S. Lee, C. Li, S. Majumder, O. Maksymets, R. Martín-Martín, R. Mottaghi, S. Raychaudhuri, M. Roberts, S. Savarese, M. Savva, M. Shridhar, N. Sünderhauf, A. Szot, B. Talbot, J. B. Tenenbaum, J. Thomason, A. Toshev, J. Truong, L. Weihs, and J. Wu, "Retrospectives on the embodied ai workshop," 2022.
- [10] D. Batra, A. Gokaslan, A. Kembhavi, O. Maksymets, R. Mottaghi, M. Savva, A. Toshev, and E. Wijmans, "Objectnav revisited: On evaluation of embodied agents navigating to objects," 2020.
- [11] M. Savva, A. Kadian, O. Maksymets, Y. Zhao, E. Wijmans, B. Jain, J. Straub, J. Liu, V. Koltun, J. Malik, *et al.*, "Habitat: A platform for embodied ai research," in *Proceedings of the IEEE/CVF International Conference on Computer Vision*, 2019, pp. 9339–9347.
- [12] Y. Liang, B. Chen, and S. Song, "Sscnav: Confidence-aware semantic scene completion for visual semantic navigation," in *2021 IEEE international conference on robotics and automation (ICRA)*. IEEE, 2021, pp. 13 194–13 200.
- [13] M. Deitke, E. VanderBilt, A. Herrasti, L. Weihs, K. Ehsani, J. Salvador, W. Han, E. Kolve, A. Kembhavi, and R. Mottaghi, "Proctor: Large-scale embodied ai using procedural generation," *Advances in Neural Information Processing Systems*, vol. 35, pp. 5982–5994, 2022.
- [14] A. Khandelwal, L. Weihs, R. Mottaghi, and A. Kembhavi, "Simple but effective: Clip embeddings for embodied ai," in *Proceedings of the IEEE/CVF Conference on Computer Vision and Pattern Recognition*, 2022, pp. 14 829–14 838.
- [15] E. Wijmans, A. Kadian, A. Morcos, S. Lee, I. Essa, D. Parikh, M. Savva, and D. Batra, "Dd-ppo: Learning near-perfect pointgoal navigators from 2.5 billion frames," *arXiv preprint arXiv:1911.00357*, 2019.
- [16] J. Ye, D. Batra, A. Das, and E. Wijmans, "Auxiliary tasks and exploration enable objectgoal navigation," in *Proceedings of the IEEE/CVF International Conference on Computer Vision*, 2021, pp. 16 117–16 126.
- [17] K. Yadav, A. Majumdar, R. Ramrakhya, N. Yokoyama, A. Baevski, Z. Kira, O. Maksymets, and D. Batra, "Ovrl-v2: A simple state-of-art baseline for imagenav and objectnav," *arXiv preprint arXiv:2303.07798*, 2023.
- [18] R. Ramrakhya, D. Batra, E. Wijmans, and A. Das, "Pirlnav: Pretraining with imitation and rl finetuning for objectnav," in *Proceedings of the IEEE/CVF Conference on Computer Vision and Pattern Recognition*, 2023, pp. 17 896–17 906.
- [19] D. S. Chaplot, D. P. Gandhi, A. Gupta, and R. R. Salakhutdinov, "Object goal navigation using goal-oriented semantic exploration," *Advances in Neural Information Processing Systems*, vol. 33, pp. 4247–4258, 2020.
- [20] S. K. Ramakrishnan, D. S. Chaplot, Z. Al-Halah, J. Malik, and K. Grauman, "Poni: Potential functions for objectgoal navigation with interaction-free learning," in *Proceedings of the IEEE/CVF Conference on Computer Vision and Pattern Recognition*, 2022, pp. 18 890–18 900.
- [21] A. J. Zhai and S. Wang, "Peanut: Predicting and navigating to unseen targets," in *Proceedings of the IEEE/CVF International Conference on Computer Vision*, October 2023, pp. 10926–10935.
- [22] S. K. Ramakrishnan, A. Gokaslan, E. Wijmans, O. Maksymets, A. Clegg, J. Turner, E. Undersander, W. Galuba, A. Westbury, A. X. Chang, M. Savva, Y. Zhao, and D. Batra, "Habitat-matterport 3d dataset (hm3d): 1000 large-scale 3d environments for embodied ai," 2021.
- [23] R. Ramrakhya, E. Undersander, D. Batra, and A. Das, "Habitat-web: Learning embodied object-search strategies from human demonstrations at scale," in *Proceedings of the IEEE/CVF Conference on Computer Vision and Pattern Recognition*, 2022, pp. 5173–5183.
- [24] M. Zhu, B. Zhao, and T. Kong, "Navigating to objects in unseen environments by distance prediction," in *2022 IEEE/RSJ International Conference on Intelligent Robots and Systems*. IEEE, 2022, pp. 10 571–10 578.
- [25] H. Luo, A. Yue, Z.-W. Hong, and P. Agrawal, "Stubborn: A strong baseline for indoor object navigation," 2022.
- [26] J. Zhang, L. Dai, F. Meng, Q. Fan, X. Chen, K. Xu, and H. Wang, "3d-aware object goal navigation via simultaneous exploration and identification," in *Proceedings of the IEEE/CVF Conference on Computer Vision and Pattern Recognition*, June 2023, pp. 6672–6682.
- [27] G. Georgakis, B. Bucher, K. Schmeckpeper, S. Singh, and K. Daniilidis, "Learning to map for active semantic goal navigation," *arXiv preprint arXiv:2106.15648*, 2021.
- [28] M. Engelcke, D. Rao, D. Z. Wang, C. H. Tong, and I. Posner, "Vote3deep: Fast object detection in 3d point clouds using efficient convolutional neural networks," in *2017 IEEE International Conference on Robotics and Automation*. IEEE, 2017, pp. 1355–1361.
- [29] B. Graham, M. Engelcke, and L. van der Maaten, "3d semantic segmentation with submanifold sparse convolutional networks," in *Proceedings of the IEEE Conference on Computer Vision and Pattern Recognition*, June 2018.
- [30] H. Tang, S. Yang, Z. Liu, K. Hong, Z. Yu, X. Li, G. Dai, Y. Wang, and S. Han, "Torchsparse++: Efficient training and inference framework for sparse convolution on gpus," in *IEEE/ACM International Symposium on Microarchitecture (MICRO)*, 2023.
- [31] K. He, G. Gkioxari, P. Dollár, and R. Girshick, "Mask r-cnn," in *Proceedings of the IEEE International Conference on Computer Vision*, 2017, pp. 2961–2969.
- [32] T. K. Ho, "Random decision forests," in *Proceedings of 3rd International Conference on Document Analysis and Recognition*, vol. 1. IEEE, 1995, pp. 278–282.
- [33] J. A. Sethian, "Fast marching methods," *SIAM review*, vol. 41, no. 2, pp. 199–235, 1999.
- [34] K. Yadav, S. K. Ramakrishnan, J. Turner, A. Gokaslan, O. Maksymets, R. Jain, R. Ramrakhya, A. X. Chang, A. Clegg, M. Savva, E. Undersander, D. S. Chaplot, and D. Batra, "Habitat challenge 2022," <https://aihabitat.org/challenge/2022/>, 2022.
- [35] G. Lemaître, F. Nogueira, and C. K. Aridas, "Imbalanced-learn: A python toolbox to tackle the curse of imbalanced datasets in machine learning," *Journal of Machine Learning Research*, vol. 18, no. 17, pp. 1–5, 2017. [Online]. Available: <http://jmlr.org/papers/v18/16-365.html>
- [36] H. Zhao, J. Shi, X. Qi, X. Wang, and J. Jia, "Pyramid scene parsing network," in *Proceedings of the IEEE CConference on Computer Vision and Pattern Recognition*, 2017, pp. 2881–2890.
- [37] P. Ren, Y. Xiao, X. Chang, P.-Y. Huang, Z. Li, X. Chen, and X. Wang, "A comprehensive survey of neural architecture search: Challenges and solutions," *ACM Computing Surveys (CSUR)*, vol. 54, no. 4, pp. 1–34, 2021.
- [38] T. Elsken, J. H. Metzen, and F. Hutter, "Neural architecture search: A survey," *Journal of Machine Learning Research*, vol. 20, no. 55, pp. 1–21, 2019.
- [39] T. Akiba, S. Sano, T. Yanase, T. Ohta, and M. Koyama, "Optuna: A next-generation hyperparameter optimization framework," in *The 25th ACM SIGKDD International Conference on Knowledge Discovery & Data Mining*, 2019, pp. 2623–2631.